Capacity analysis of underwater acoustic MIMO communications

Pierre-Jean BOUVET and Alain LOUSSERT
Underwater Acoustics Lab
ISEN Brest
C.S. 42807, 29228 BREST cedex 2 - FRANCE
Email: pierre-jean.bouvet@isen.fr

***Abstract*—First introduced in the field of radio communications, Multi-Input Multi-Output (MIMO) principle consists of transmitting digital data from N_t transmitters to N_r receivers within the same frequency band. During the last decade, theoretical works and real-life experiments in wireless local area and cellular networks have demonstrated and confirmed that MIMO was a breakthrough in digital communications. Recently, MIMO principle has been applied to underwater acoustic communications (UAC) with promising results. However, only few work have been already done on the expected gain of MIMO over underwater channel. Main objective of our paper is on the one hand to quantify theoretically the MIMO gain in underwater acoustic channel by using Shannon capacity analysis and on the other hand to give guidelines to optimize MIMO underwater system with respect to capacity maximization.**

I. Introduction

Initially introduced during world war II for military needs, underwater communications have today a growing number of civil and commercial applications such as remote control in off-shore oil industry, pollutions monitoring in environmental systems, collection of scientific data recorded at ocean-bottom stations, communication between divers or underwater vehicles and mapping of the ocean floor for detection of objects as well as for the discovery of new resources. As electromagnetic waves cannot propagate over long distances in seawater, underwater acoustic is the core enabling technology for such applications. However underwater acoustic channel characteristics such as fading, extended multi-path bandwidth limitations or reverberation pose significant challenges to development of effective UAC systems [1] [2] [3].

On the other front, data rate required for UAC applications is continuously growing with the introduction of high quality images, real-time video as well as the deployment of autonomous underwater networks such as ad-hoc deployable sensor networks or autonomous fleets of cooperating unmanned undersea vehicles (UUV) [4]. Since underwater acoustic channel is very selective in frequency, transmission throughput could not be increased by simply increasing transmission bandwidth. We can find a similar paradigm in wireless communication for which there is a huge requirement in high speed communication whereas usable bandwidth is restricted by frequency allocation law. In radio frequency field, this bandwidth limitation has been overcome by the introduction of MIMO techniques which provides substantial gain in data rate while keeping the same transmission bandwidth [5] [6] [7] [8]. In the past years, the contribution of MIMO to UAC systems has been deeply investigated via spatial modulation [9] or multi-carrier modulation [10]. Initial simulation and experimental results demonstrate large gain over conventional single input single output (SISO) but these results are strongly linked to the chosen modulation scheme and receiver algorithm as well as underwater channel environment.

Coming from the information theory, the channel capacity represents the tightest upper bound on the amount of information that can be reliably transmitted over a communications channel. Thus the channel capacity of a given channel is the limiting information rate (in units of information per unit time) that can be achieved with arbitrarily small error probability regardless of the receiver algorithm [11]. One of the questions that arises naturally is what is the maximum rate that a MIMO underwater acoustic channel can theoretically supported and how large is the MIMO contribution. While research has been extremely active on assessing capacity of wireless radio transmission, only few analysis have been reported mostly focusing on SISO channel [12] [13]. Within the few available reference dealing with MIMO underwater acoustic capacity, [14] provides capacity estimation using simulated and experimental data but under the assumption transmitter has a knowledge of the channel transfer function which is not really feasible in UAC. Authors of [15] carry out capacity results both for SISO and MIMO channel but using a broadband propagation model that does not reflect frequency selectivity brought by multi-path propagation. Intention of our paper is to provide a full theoretical analysis of the MIMO underwater capacity under the assumption of shallow water acoustic (SWA) channel by taking into account both underwater propagation and multi-path bandwidth limitation in order to give an accurate approximation of maximum theoretical data rate expected from a real-life MIMO UAC system.

Paper is organized as follows : section II describes the underwater acoustic channel and how the latter affects a

978-1-4244-5222-4/10/$26.00 ©2010 IEEE

transmitted signal. In section III, we introduce a mathematical model of SWA channel based on ray-theory. In section IV, we start from theoretical expression of the MIMO capacity in order to derive an expression of MIMO SWA capacity. Finally section V provides extended results covering several MIMO configuration and channel parameters.

II. Channel characteristics

When compared to electromagnetic propagation through the atmosphere, underwater acoustic propagation is characterized by significant frequency dependent perturbations and relatively slow speed of propagation. Transmission loss and noise are the principal factors determining functional point of a underwater communication system, however the slow speed of wave propagation leads to time-varying multipath phenomenon that also influences system design and generally imposes severe limitations on the system performance.

A. Transmission loss

The attenuation mechanisms that affects underwater acoustic signal can be viewed as sum of three terms : the spreading loss, absorption loss and reflection loss.

The spreading losses are due to the expansion of the fixed amount of transmitted energy over a larger area as the signal propagates away from its source. It's admitted that the energy decays at a rate of l^{-k} where l is the distance and k the spreading factor describing the geometry of propagation (its commonly used values are $k = 2$ for spherical spreading, $k = 1$ for cylindrical spreading and $k = 1.5$ for the so-called practical spreading).

The second mechanism of signal loss, called absorption loss, results from the conversion of the energy of the propagating wave into heat. In case of under-sea acoustic transmission, the absorption loss is strongly linked to the wave frequency, such that the signal energy decay due to absorption loss is proportional to $\exp(-\alpha(f)l)$ where $\alpha(f)$, referred as the absorption coefficient, is an increasing function of frequency. The absorption loss can be expressed empirically using the Thorp's formula which gives $\alpha(f)$ in dB/km for a given frequency f in kHz [16] [17]:

$$10 \log \alpha(f) = 0.11 \frac{f^2}{1+f^2} + 44 \frac{f^2}{4100+f^2} + 2.75 \cdot 10^{-4} f^2 + 0.003 \quad (1)$$

This formula is valid for $f > 400$ kHz. For lower frequencies, the formula becomes:

$$10 \log \alpha(f) = 0.002 + 0.11 \frac{f^2}{1+f^2} + 0.011 f^2 \quad (2)$$

By hitting the sea-surface, sea-bottom or another under-sea object, the sound wave is partially or totally reflected depending on the wave frequency, the sound speed and the obstacle type. The reflection loss for path p is denoted as Γ_p and will be described more in depth is section III.

As a result, the total path loss that occurs in a under-sea acoustic channel is equal to $\Gamma_p / \sqrt{A(l,f)}$ where $A(l,f)$ is the sum of spreading and absorption loss:

$$10 \log A(l,f) = k \cdot 10 \log l + l \cdot 10 \log \alpha(f) \quad (3)$$

B. Noises

There are several important natural sources of ambient noise in the ocean at frequencies of interest for acoustic communications. Usually four sources are considered: turbulence, shipping, waves and thermal noise.These four noise components can be modeled by a colored Gaussian noise with following empirical power spectral density (p.s.d.) given in dB re μ per Hz as a function of frequency in kHz [18] [13]:

$$10 \log N_t(f) = 17 - 30 \log f$$
$$10 \log N_s(f) = 40 + 20(s - 0.5) + 26 \log f - 60 \log(f + 0.03)$$
$$10 \log N_w(f) = 50 + 7.5 w^{1/2} + 20 \log f - 40 \log(f + 0.4)$$
$$10 \log N_{th}(f) = -15 + 20 \log f$$

where s is the shipping activity whose value ranges between 0 and 1 for low and high activity respectively whereas w is the wind speed expressed in m/s. The overall p.s.d. of the ambient noise is noted $N(f)$ and expressed as the sum of the four above mentioned noise components:

$$N(f) = N_t(f) + N_s(f) + N_w(f) + N_{th}(f) \quad (4)$$

This strong frequency dependency of the ambient noise is one of major factor considered when selecting frequency bands for underwater acoustics transmission.

C. Multi-paths propagation

In most environments and at the frequency of interest for communications signals, the underwater channel results in multiple propagation paths from each source to receiver. In the first place, the multi-paths spread depends in the the transmission link configuration designated as horizontal or vertical. While vertical links are subjected to little time dispersion, horizontal channels may exhibit a very long delay spread. Mechanism of multi-paths formation are also strongly linked to the ocean depth: in case of deep water, multi-paths are formed by ray bending which occurs because the rays of sound tend to reach region of lower propagation speed whereas in case of shallow water environment (such as in the littoral region or the region of continental shelves), multi-path mechanism consists of reflections on surface-bottom bounces in addition to a possible direct path. The definition of shallow and deep water is not a strict one, but it is generally assumed that shallow water corresponds to a water depth less than 100 m. In the following we will focus on horizontal link within SWA channel which presents a very challenging communications scenario regarding the multiple propagation path effects. Moreover we assumes a constant water temperature within the whole water column which implies a constant sound speed (isovelocity).

In a digital communication system, multi-paths propagation causes inter-symbol interference (ISI) that have to be carefully treated at the receiver side in order to guarantee acceptable performance [19]. As result, the design of underwater communication systems is accompanied by the use of propagation model for predicting the multi-path configuration. Ray theory and the theory of normal modes provide basis for such propagation modeling [1]. At high frequencies, ray tracing is an appropriate model and is commonly used to determine the coarse multi-paths structure of the channel. In the following we will consider medium range transmission (≤ 5 km) which usually requires high frequency and justifies the use of ray model as the basis of our channel propagation model.

D. Time-variation

Each propagation path may be also characterized by a random fluctuation component due to the scattering on moving sea-surface (waves or bubbles). Motion of the reflection points results in the Doppler spreading of the reflected signals leading to time-varying impulse response of the channel. One can note that time-varying effect is present within the underwater channel regardless an eventual motion of transmitter or receiver. For simplicity reason, we'll assume in our study a calm sea-surface such that arrivals of surface scattered paths in the impulse response is both fairly stable and localized in delay.

III. MIMO CHANNEL MODEL

In this section we first develop a mathematical model for signal propagation through a SWA channel based on ray tracing model derived from ocean physics. Then we provide a filter-based representation of the channel and finally we extend this model to MIMO architecture.

A. Propagation model based on ray tracing

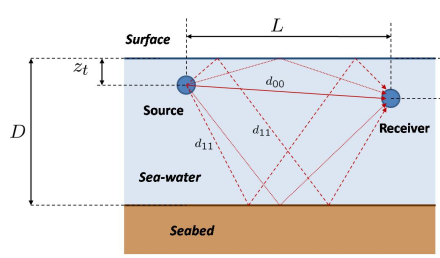

Fig. 1. Channel representation

In the ray propagation model, sound energy is conceptualized as propagating along *rays*, which are straight lines in the case of fluid medium with constant sound speed (isovelocity) [20]. These rays are partially reflected and refracted when they encounter a discontinuity in sound speed. We model the SWA channel as a wave guide consisting of an isovelocity layer (represented by the seawater) between two isovelocity half spaces: air and seabed [21]. The isovelocity assumption is justified as shallow water channel are usually well mixed and have relatively small increase in pressure over the depth of the water column.

Let L be the transmission range, D the water depth, z_t and respectively z_r be the depth of the transmitter and the receiver respectively. The distance traveled by the sound along various rays can be computed using geometrical approach. Let d_{sb} be the distance along an upward originating eigenrays with s surface reflections and b bottom reflections. The distance along a direct ray d_{00} is simply equal to:

$$d_{00} = \sqrt{R^2 + (z_t - z_r)^2} \tag{5}$$

In the general case, if $0 \leq s - b \leq 1$, the distance becomes

$$d_{sb} = \sqrt{R^2 + (2bD + z_t - (-1)^{s-b} z_r)^2} \tag{6}$$

Inversely, if $0 \leq b - s \leq 1$, we have:

$$d_{sb} = \sqrt{R^2 + (2bD - z_t + (-1)^{b-s} z_r)^2} \tag{7}$$

Attenuation coefficient due to reflection on surface denoted Γ^+ is relatively small in magnitude since the impedance mismatch between the seawater and air. If the sea is calm, reflection coefficient tends to perfect reflection value 1. If the sea surface is rough (due to waves), a small loss will be incurred for every surface interaction. This loss is modeled by a constant coefficient L_{SS}.

On the seabed boundary, the coefficient reflection depends on the impedance variation from water to seabed. Such coefficient estimation is given in [21] using Rayleigh reflexion law:

$$\Gamma^- = \left| \frac{\frac{\rho_1}{\rho} cos\theta - \sqrt{(\frac{c}{c_1})^2 - sin^2\theta}}{\frac{\rho_1}{\rho} cos\theta + \sqrt{(\frac{c}{c_1})^2 - sin^2\theta}} \right| \tag{8}$$

where ρ and ρ_1 are density of water and sea-bed respectively, c and c_1 are sound speed in water and sea-bed respectively whereas θ is the incidence angle of reflected wave that can be computed from the ray d_{sb} as follows if $0 \leq s - b \leq 1$ [21]:

$$\theta_{sb} = \tan^{-1}\left(\frac{L}{2bD + z_t - (-1)^{s-b} z_r}\right) \tag{9}$$

and if $0 \leq b - s \leq 1$:

$$\theta_{sb} = \tan^{-1}\left(\frac{L}{2bD - z_t + (-1)^{b-s} z_r}\right) \tag{10}$$

Additional reflection losses due to rough or absorbing sea bottom is modeled by a constant coefficient L_{SB}. Finally the total reflection loss for a path with s surface and b bottom reflections is equal to:

$$\Gamma_{sb} = \left(\Gamma^+ \cdot L_{SS}\right)^s \cdot \left(\Gamma^- \cdot L_{SB}\right)^b \tag{11}$$

The arrival time of each ray τ_{sb} is easily computed from the distance along the ray and sound speed:

$$\tau_{sb} = \frac{d_{sb}}{c} \tag{12}$$

B. FIR tap representation

By traveling from transmitter to receiver, each ray follows a path of length d_{sb} with arrival time τ_{sb} and an attenuation of $\Gamma_{sb}/\sqrt{A(d_{sb}, f)}$. The SWA channel is modeled by taking account all possible paths and result in an Finite Impulse Response (FIR) filter with following transfer function [21]:

$$
\begin{aligned}
H(f) \quad &= \quad \frac{1}{\sqrt{A(d_{00}, f)}} e^{-j2\pi f \tau_{00}} \\
&+ \sum_{s=1}^{+\infty} \sum_{b=s-1}^{s} \frac{\Gamma_{sb}}{\sqrt{A(d_{sb}, f)}} e^{-j2\pi f \tau_{sb}} \\
&+ \sum_{b=1}^{+\infty} \sum_{s=b-1}^{b} \frac{\Gamma_{sb}}{\sqrt{A(d_{sb}, f)}} e^{-j2\pi f \tau_{sb}}
\end{aligned}
$$

For practical computation, we'll assume that number of reflections on surface and sea-bottom is finite and equal to s_{max} and b_{max} respectively. Total number of paths is then equal to P with:

$$P = 1 + 2s_{max} + 2b_{max} \tag{13}$$

The channel transfer function can be rewritten as a closed-from expression:

$$H(f) = \sum_{p=0}^{P-1} \frac{\Gamma_p}{\sqrt{A(l_p, f)}} e^{-j2\pi f \tau_p} \tag{14}$$

where Γ_p , $A(d_p)$ and τ_p are the total reflection loss, the medium attenuation, and the arrival time of path p respectively. As an example, figure 2 and 3 represents the channel impulse response (CIR) and frequency response obtained of the modeled SWA channel with parameters described in section V. The spectrum response exhibits a slow decrease in frequency explained by the frequency dependency of $A(l, f)$.

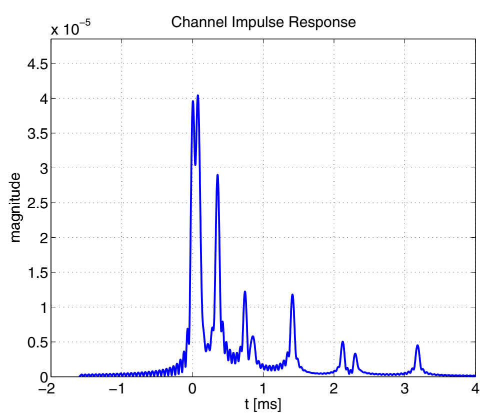

Fig. 2. Example of Channel Impulse Response (CIR) of SWA channel

C. Extension to MIMO

We consider now a MIMO underwater transmission architecture with N_t transmit hydrophones and N_r receive hydrophones. On the transmit and receive sides, each hydrophone pair has a vertical and constant separation of Δz_t and Δr_t respectively. The transmitter and receiver depths z_t and z_r correspond to the middle of each array as shown in figure 4. The MIMO array is placed in vertical direction in order to maximize delay spread difference between each sub-channels and thus minimize spatial correlation.

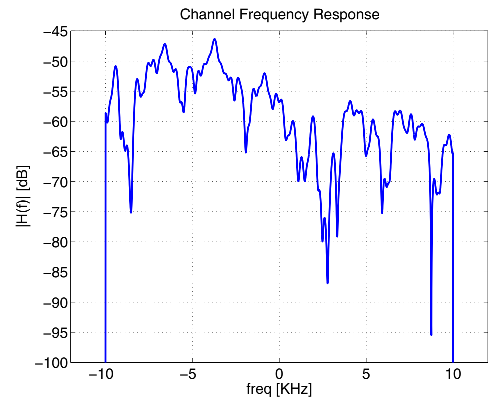

Fig. 3. Example of frequency response of SWA channel

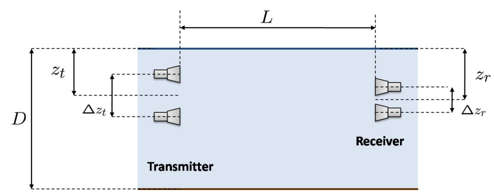

Fig. 4. MIMO SWA Channel representation

The MIMO channel is modeled by $N_t \times N_r$ sub-channels, where each sub-channel corresponds to the SWA channel model described in previous section. As a result, the transfer function of sub-channel linking hydrophone $m \in [1, N_t]$ to hydrophone $n \in [1, N_r]$ denoted $H_{mn}(f)$ is simply derived from equation (14) as follows:

$$H_{mn}(f) = \sum_{p=0}^{P-1} \frac{\Gamma_p}{\sqrt{A(d_{p,mn}, f)}} e^{-j2\pi f \tau_{p,mn}} \tag{15}$$

where $d_{p,mn}$ is the distance along the p-th path of sub-channel mn and $\tau_{p,mn} = d_{p,mn}/c$. For simplicity, we assume each sub-channel to experience the same path number P. In order to take into account geometry of the MIMO array, each distance $d_{p,mn}$ is computed by replacing in (5), (6), (7), (9) and (10) z_t and z_r by z_{tm} and z_{rn} respectively:

$$z_t \rightarrow z_{tm} = z_t - (N_t + 1 - 2m)\frac{\Delta z_t}{2} \tag{16}$$

$$z_r \rightarrow z_{rn} = z_r - (N_r + 1 - 2n)\frac{\Delta z_r}{2} \tag{17}$$

Finally the whole MIMO channel is represented by the following $N_r \times N_t$ channel matrix:

$$\mathbf{H}(f) = \begin{bmatrix} H_{11}(f) & \dots & H_{N_t1}(f) \\ \vdots & \ddots & \vdots \\ H_{1N_r}(f) & \dots & H_{N_tN_r}(f) \end{bmatrix}_{N_r \times N_t} \quad (18)$$

IV. Capacity Computation

The channel capacity represents the maximum amount of information that can be reliably transmitted over a communications channel [11]. This quantity is defined as the maximization of the average mutual information $\mathcal{I}(\mathbf{x}, \mathbf{y})$ between input signal $\mathbf{x}$ and output signal $\mathbf{y}$ of the channel over the choice of the distribution of $\mathbf{x}$.

In the following, we derive the capacity formula of SWA MIMO channel by taking into account all characteristics developed in section II. In order to evaluate relatively the SWA MIMO capacity, we also remind some useful capacity bounds both for SISO and MIMO channel.

A. SWA MIMO Channel

In case of deterministic MIMO, E. Telatar derived the general expression of the MIMO capacity [5]:

$$C = \log_2 \left(\mathbf{I}_{N_t} + \frac{SNR}{N_t} \mathbf{H} \mathbf{R_{ss}} \mathbf{H}^H \right) \quad \text{[bits/s/Hz]} \quad (19)$$

where $\mathbf{I}_{N_t}$ is the $N_t \times N_t$ identity matrix, SNR is the signal-to-noise ratio, $\mathbf{H}$ is MIMO matrix, $\mathbf{R_{ss}}$ is the covariance matrix of input signal and $(.)^H$ denotes the transpose conjugate operand. As demonstrated by C. E. Shannon in the SISO case, E. Telatar shown that mutual information is maximized by choosing input signal vector $\mathbf{s}$ as independent and zero mean Gaussian samples [5].

Let be λ_i the eigen values of $\mathbf{H}$ with $0 \le i < r$ where $r = \text{rank}(\mathbf{H})$, expression (19) can be expanded as [5]:

$$C = \sum_{i=0}^{r-1} \left(1 + \frac{SNR}{N_t} \lambda_i \right) \quad (20)$$

Since the right part of latest expression is homogeneous to a SISO capacity (see [11]), the MIMO capacity can be viewed as a sum of r SISO capacities. The MIMO capacity is thus maximized when rank of $\mathbf{H}$ reaches its maximum value which is equal to $\max(r) = \min(N_t, N_r)$. This leads to the well-known property of MIMO system: at it's bests MIMO capacity gain is increasing linearly with minimum number of transmit and receive sensors [6]. And more generally, advantageous of MIMO depends on matrix $\mathbf{H}$, the larger rank and eigenvalues $\mathbf{H}\mathbf{H}^H$ have, the more MIMO capacity we have [7].

If the channel could be known at the transmit side (with for example a feedback loop), capacity could be maximized by adjusting the covariance matrix R_{SS} of transmit signal with water-filling techniques [5] [6]. However in UWA communications, the high variability and latency of the channel makes difficult any feedback from receiver to transmitter such as channel matrix is usually assumed as unknown for the transmitter.

In the absence of channel state information at the transmitter it is reasonable to choose the transmit signal $\mathbf{s}$ to be white in space and in frequency directions: $\mathbf{R_{ss}} = \mathbf{I}_{N_t}$. The total transmit power P_s is thus assumed to be uniformly distributed over the bandwidth B and the N_t transmit hydrophones such as the power profile density (p.s.d.) of signal transmitted from hydrophone $m \in [1, N_t]$ is expressed as:

$$S(f) = \frac{P_S}{B \cdot N_t} \quad , \forall f \in \left[f_0 - \tfrac{B}{2}, f_0 + \tfrac{B}{2} \right] \quad (21)$$

where f_0 is center carrier frequency around which the signal is transmitted. At receive side, the total power receive from hydrophone $n \in [1, N_r]$ is equal to:

$$P_{Rn} = \int_{f_0 - B/2}^{f_0 + B/2} R_n(f) df \quad (22)$$

where R_n is received signal p.s.d. viewed by hydrophone n:

$$R_n(f) = \sum_{m=1}^{N_t} |\mathbf{H}_{mn}(f)|^2 S(f) \quad (23)$$

On the other front, the total noise power is:

$$P_N = \int_{f_0 - B/2}^{f_0 + B/2} N(f) df \quad (24)$$

As a result the the signal-to-noise ratio viewed at receive hydrophone $n \in [1, N_r]$ can be expressed as:

$$SNR_n = \frac{P_{Rn}}{P_N} \quad (25)$$

whereas the SNR p.s.d. is:

$$SNR_n(f) = \frac{R_n(f)}{N(f)} \quad (26)$$

Previous capacity formulas are provided under the assumption that MIMO channel described by matrix $\mathbf{H}$ is flat fading. Let now consider a tone f within the transmit bandwidth for which the SWA channel can be considered flat, formula (19) can be rewritten as follows:

$$C(f) = \log_2 \left(\mathbf{I}_{N_t} + \frac{S(f)}{N_t \cdot N(f)} \mathbf{H}(f) \mathbf{H}(f)^H \right) \quad (27)$$

where $N(f)$ is the underwater noise p.s.d. described in section II whereas $\mathbf{H}(f)$ is the SWA channel transfer function introduced in section III. The total channel capacity is obtained by integrating $C(f)$ over the transmit bandwidth B:

$$C = \int_{f_0 - B/2}^{f_0 + B/2} C(f) df \quad \text{[bits/s/Hz]} \quad (28)$$

B. SWA SISO Channel

The Shannon capacity of the SWA SISO channel is obtained by particularizing (27) and (28) to the single hydrophone case i.e. $N_t = 1$ and $N_r = 1$ leading to the following expression:

$$C_0 = \int_{f_0-B/2}^{f_0+B/2} \log_2\Big(1 + \frac{S_0(f)}{N(f)}\big|H_{11}(f)\big|^2\Big) df \quad \text{[bits/s/Hz]} \tag{29}$$

where the p.s.d. of the transmitted signal becomes:

$$S_0(f) = \frac{P_S}{B} \quad , \forall f \in \Big[f_0 - \tfrac{B}{2}, f_0 + \tfrac{B}{2}\Big] \tag{30}$$

Please note that more detailed results on capacity of SWA SISO channel can be found in [13].

C. Upper bounds

In the absence of channel knowledge at the transmit side, capacity of an arbitrary SISO channel is bounded by the so-called AWGN capacity obtained over a memoryless additive white Gaussian noise (AWGN) channel and expressed in [11] as:

$$\bar{C}_0 = \log_2\Big(1 + \frac{P_S}{P_N}\Big) \quad \text{[bits/s/Hz]} \tag{31}$$

By using (20) and (31), one can demonstrated capacity of an arbitrary MIMO channel is bounded by:

$$\bar{C} = \min(N_t, N_r) \cdot \log_2\Big(1 + \frac{P_S}{P_N}\Big) \quad \text{[bits/s/Hz]} \tag{32}$$

This result could be interpreted as the optimum MIMO scheme were equivalent to $\min(N_t, Nr)$ AWGN channels operating at separate bandwidths.

D. Rayleigh bounds

In wireless communications, a usual channel model consists of modeling frequency fading as i.i.d. random Rayleigh coefficients. Each channel flat coefficient h_{mn} of matrix $\mathbf{H}$ are modeled as uncorrelated complex Gaussian samples with zero mean and unit variance. Channel capacity is computed by taking the expectation of instantaneous capacity over the realization of $\mathbf{H}$:

$$\tilde{C} = \mathcal{E}_{\mathbf{H}}\Big[\log_2\Big(\mathbf{I}_{N_t} + \frac{P_S}{N_t P_N}\mathbf{H}\mathbf{H}^H\Big)\Big] \quad \text{[bits/s/Hz]} \tag{33}$$

Such capacity is called ergodic since it's assumed that th channel transfer function obeys to an ergodic random process. As previously, the equivalent SISO capacity is obtained by particularizing to the single hydrophone case:

$$\tilde{C}_0 = \mathcal{E}_{\mathbf{h_{oo}}}\Big[\log_2\Big(\mathbf{I}_{N_t} + \frac{P_S}{N_t P_N}|h_{11}|^2\Big)\Big] \quad \text{[bits/s/Hz]} \tag{34}$$

V. Simulation Results

A. Simulation set-up

Channel parameters chosen for simulation works are summarized in Table I. These parameters are derived from MIMO experiments made in [10]. SWA channel capacities are numerically evaluated using (28) and (29) with a frequency resolution equals to $\Delta f = 7.6$ Hz. We use a quite high frequency resolution in order to take into account large frequency fadings brought by SWA channel.

TABLE I
SIMULATION PARAMETERS

Letter	Name	Default value
F_0	Carrier frequency	32 kHz
B	Signal Bandwidth	12 kHz (Variable)
F_s	Sampling frequency	500 kHz
Δf	frequency resolution	7.6 Hz
L	Range	1500 m (variable)
D	Water depth	20 m (variable)
N_t	Number on transmit hydrophones	2
N_r	Number on receive hydrophones	2
z_t	Transmit array depth	9 m
Δz_t	Vertical separation of transmit array	0.6 m (variable)
z_r	Receive array depth	9 m
Δz_r	Vertical separation of receive array	0.6 m (variable)
k	Spreading factor	1.5
c	Sound speed in water	1500 m/s
ρ	Water density	1023 kg/m^3
c_1	Sound speed in sea-bottom	1650 m/s
ρ_1	Sea-bottom density	1500 kg/m^3
L_{SS}	Absorption loss at sea-surface	-0.5 dB
L_{SB}	Absorption loss at sea-bottom	-3 dB

B. Capacity of the SWA MIMO channel

Figure 5 shows the MIMO 2×2 capacity (C) and SISO capacity (C_0) results of a SWA channel with the default parameters described in table I. As references, 2×2 AWGN capacity ($\bar{C}$), SISO AWGN capacity ($\bar{C}_0$), 2×2 Rayleigh i.i.d. capacity ($\tilde{C}$) and SISO Rayleigh i.i.d. capacity ($\tilde{C}_0$) are also plotted in the same figure. First, we can observe the large capacity gain brought by MIMO architecture. As an example for $SNR = 15$ dB, SWA channel capacity is increased from 3.9 to 8 bits/s/Hz representing a maximum MIMO throughput of 96 kbits/s with the chosen bandwidth of 12 kHz. Thus the MIMO gain is about 103 % demonstrating the SWA capacity is increasing linearly with $\min(N_t, N_r)$ as shown in section IV. As a result, larger could be obtained by increasing the number of hydrophones at transmit and receive side.

By comparing with the Rayleigh bounds, one can see that C curve is quite close to $\tilde{C}$ whereas C_0 is lower than $\tilde{C}_0$. For the SISO case, capacity result confirms the limitation to use a Rayleigh fading model to represent the SWA channel as already pointed out in literature by experimental results [20]. However due to the high fading diversity brought by the multi-sensors approach, MIMO SWA channel tends to approach MIMO Rayleigh i.i.d. model. Finally, both SISO and MIMO SWA curves are staying quite far from AWGN bounds which is note very surprising since SWA channel remains a very challenging and difficult communication channel.

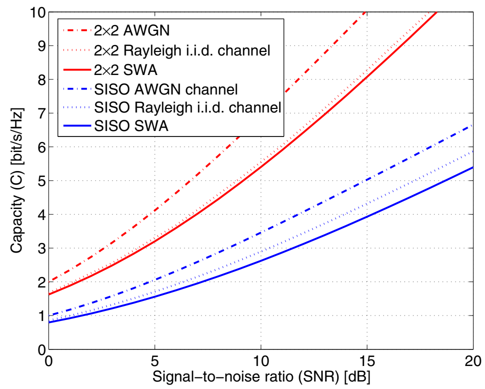

Fig. 5. MIMO 2×2 and SISO capacities as function of SNR. Default parameters are set for SWA channel model.

C. Bandwidth and communication range

As described extensively in section II, sound propagation in water is very sensitive to the wave frequency. This dependency is illustrated by the fact that $SNR_n(f)$ includes on the one hand a frequency dependent part represented by quantity $A(l,f)N(f)$ also called in the literature AN product [13] and on the other hand a frequency fading coefficient $\exp(-j2\pi f\tau_p)$. In a MIMO configuration, this dependence is illustrated in figure 6 where $SNR(f)$ expression is plotted as function of frequency for increasing values of communication range D. As in SISO case, SNR becomes more frequency selective by increasing the communication range leading to a smaller bandwidth usable for transmission. At the same time, figure 6 shows that operating frequencies are also decreasing for long range value meaning that high frequencies are dedicated for small or medium range communications. It is also interesting to notice that SNR becomes smoother for high value of D, demonstrating that for long range, the dominant factor is not longer the frequency fading but transmission loss represented by the AN product.

A second illustration is obtained by plotting in figure 7

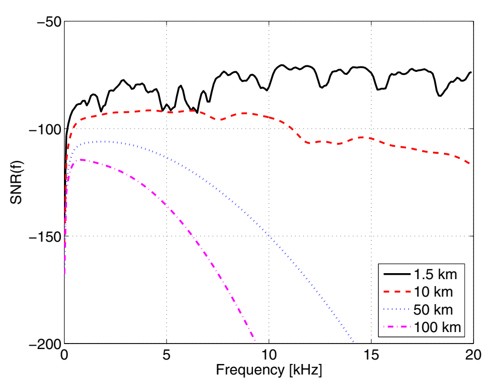

Fig. 6. $SNR(f)$ at output of 2×2 SWA channel as a function of frequency

MIMO and SISO capacities as function of D for a fixed SNR of 15 dB. As expected both SISO and MIMO SWA capacities decrease when D increases. This phenomenon is a classical feature that distinguishes an underwater acoustic system from a terrestrial radio one : UAC capacity has a strong dependency in the transmission distance [13]. However one can see that MIMO SWA capacity fades much rapidly the SISO one meaning the frequencies used for MIMO transmission have to be carefully chosen as function of the desired range.

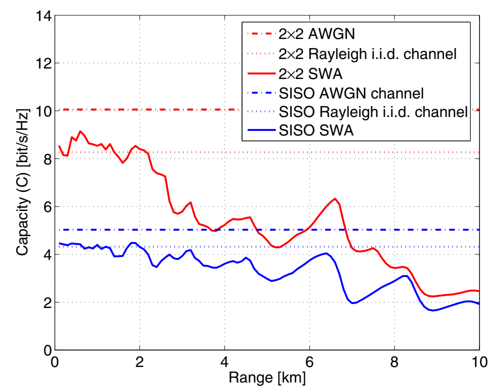

Fig. 7. MIMO and SISO Capacities as function of communication range, $SNR = 15$ dB

D. Influence of water depth

Figure 8 provides capacity results for varying value of water depth D. One can see that MIMO capacity gain is slowly decreasing as water column depth increases. The largest gain is obtained for very shallow water ($\leq$ 30 m). This result is easily explained by the fact that MIMO capacity is strongly linked to the correlation between sub-channels mathematically represented by matrix determinant of $\mathbf{HH}^H$: the lower is the spatial correlation the larger is the MIMO gain (see section IV). The lowest spatial correlation is reached in case of rich multi-paths environment which happens when channel water depth is very shallow. However some specific combinations of path delays lead to low correlation configurations which explain local maximums observed along the MIMO SWA curve.

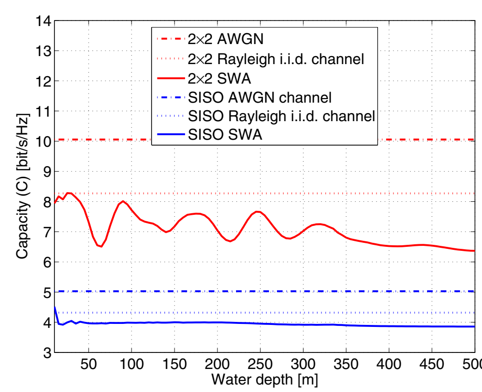

Fig. 8. MIMO and SISO Capacities as function of water depth, $SNR = 15$ dB

E. Optimizing MIMO architecture

As illustrated previously, MIMO capacity is function of the correction between each sub-channels linking each multi-sensors. Since reflection interfaces (Sea-surface and sea-bed) are situated in the vertical direction relatively to hydrophones, the lowest spatial correlation configurations are obtained with hydrophone array oriented in vertical direction. Furthermore, an easy way to ensure uncorrelated links is to space sufficiently each hydrophones within the transmit or the receive arrays as shown in figure 9 where MIMO SWA capacity is plotted as function of Δz_t and Δz_r (which are supposed to be equal). One can see that perfect uncorrellation is obtained when hydrophone separation is greater than 0.8 m. The oscillation phenomenon observed for large value of Δz_t and Δz_r is explained by the phase combination of $H_{mn}(f)$ which is linked to distance and leads to periodic variation of the correlation ratio. On the other hand it is interesting to notice that low-spaced array leads to capacity which remains larger than the SISO case. In fact, for the extreme value of $\Delta = 0$, MIMO SWA capacity is 4.8 b/s/Hz whereas SISO SWA capacity is equal to 3.93 which still represents a capacity gain of 22 %.

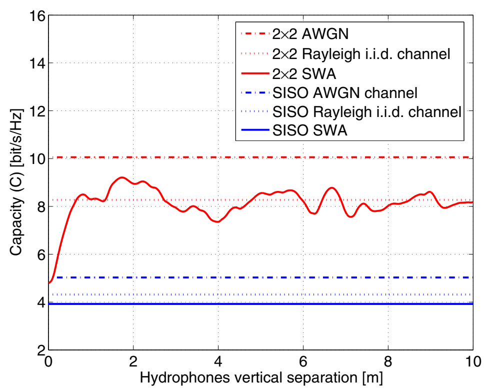

Fig. 9. MIMO and SISO Capacities as function of hydrophones vertical separation (Δz_t = Δz_r), $SNR = 15$ dB

VI. Conclusions

The primary aim of this study was to quantify and predict gain brought by MIMO technology for underwater acoustic communication. By using the ray-theory approach and under the assumption of shallow water environment, the paper provides a model of the MIMO underwater acoustic channel taking into account all the under-sea dominant perturbations. A numerical evaluation of the underwater channel capacity is then proposed leads to an accurate approximation of maximum achievable throughput for a given set of underwater communication parameters. Extensive simulation results for several transmission parameters and channel configuration show the expected MIMO gain is substantial and the capacity increase is in the same order as in wireless transmission. The study demonstrated also that some restrictions on frequencies, communication range as well as underwater environment have to be made in order to ensure MIMO capacity gain. Especially, medium range transmission over shallow water channel seems to be well a dedicated system to MIMO transmission.

With this capacity based approach, our paper gives a simple mean to provide an upper bound of the expected MIMO gain in the field of undersea acoustics and forms a useful tool to design and optimize future MIMO underwater communication system.

References

[1] R. F. W. Coates, *Underwater Acoustic Systems*. Wiley, 1989.

[2] M. Stojanovic, “Recent advances in high-speed underwater acoustic communications,” *IEEE J. Ocean. Eng.*, vol. 121, no. 2, pp. 125–136, Apr. 1996.

[3] R. S. H. Istepanian and M. Stojanovic, *Underwater acoustic digital signal processing and communication systems*. Kluwer Academic Pub., 2002.

[4] I. F. Akyildiz, D. Pompili, and T. Melodia, “Underwater acoustic sensor networks: research challenges,” *Ad Hoc Network Jorunal*, vol. 3, no. 3, pp. 257–279, 2005.

[5] E. Telatar, “Capacity of multiantenna gaussian channel,” *Bell Labs. Tech. Memo.*, Jun. 1995.

[6] G. J. Foschini, “Layered space-time architecture for wireless communication in a fading environment when using multielement antennas,” *Bell Syst. Tech. Journal*, vol. 1, pp. 41–59, Oct. 1996.

[7] D. Gesbert, M. Shafi, D. Shiu, and P. Smith, “From theory to practice: An overview of space-time coded mimo wireless systems,” *IEEE J. Sel. Areas Commun.*, Apr. 2003.

[8] A. Paulraj, A. D. Gore, R. U. Nabar, and H. Boelcskei, “An overview of MIMO communications: A key to gigabit wireless,” *Proceedings of the IEEE*, vol. 92, no. 2, pp. 198–218, Feb. 2004.

[9] D. B. Kilfoyle, J. C. Preisig, and A. B. Baggeroer, “Spatial modulation experiments in the underwater acoustic channel,” *IEEE J. Ocean. Eng.*, vol. 30, no. 2, pp. 406–415, Apr. 2005.

[10] B. Li, J. Huang, S. Zhou, K. Ball, M. Stojanovic, L. Freitag, and P. Willett, “MIMO-OFDM for high rate underwater acoustic communications,” *IEEE J. Ocean. Eng.*, vol. 34, no. 4, pp. 634–644, 2009.

[11] C. E. Shannon, “A mathematical theory of communications,” *Bell Syst. Tech. Journal*, vol. 27, pp. 379–423 and 623–656, Jul. 1948.

[12] T. J. Hayward and T. C. Yang, “Underwater acoustic communication channel capacity: A simulation study,” in *Proceedings of High Frequency Ocean Acoustics Conference*, vol. 728, 2004, pp. 114–121.

[13] M. Stojanovic, “On the relationship between capacity and distance in an underwater acoustic communication channell,” *ACM SIGMOBILE Mobile comput. and Comm. Review (M2CR)*, vol. 11, pp. 34–43, Oct. 2007.

[14] M. Zatman and B. Tracey, “Underwater acoustic mimo channel capacity,” in *Proceedings of 36th Asilomar conf.*, vol. 2, 2002, pp. 1364–1368.

[15] T. J. Hayward and T. C. Yang, “Single- and multi-channel underwater acoustic communication channel capacity: A computational study,” *Journal of the Acoustical Society of America*, vol. 122, no. 3, pp. 1652–1661, Sep. 2007.

[16] W. H. Thorp, “Analytic description of the low frequency attenuation coefficient,” *Journal of the Acoustical Society of America*, vol. 33, pp. 334–340, 1961.

[17] F. H. Fisher and V. P. Simons, “Sound absorption in seawater,” *Journal of the Acoustical Society of America*, vol. 62, pp. 558–564, 1977.

[18] R. J. Urick, *Ambient Noise in the Sea*. Peninsula Pub, 1986.

[19] J. G. Proakis, *Digital Communications*. Mc Graw Hill, 1995.

[20] X. Geng and A. Zielinski, “An eigenpath underwater acoustic communication channel model,” in *Proceedings of OCEAN’95*, vol. 2, 1995, pp. 1189–1196.

[21] M. A. Chitre, “A high-frequency warm shallow water acoustic communications channel model and measurements,” *Journal of the Acoustical Society of America*, vol. 5, no. 122, pp. 2580–2586, 2007.